PCCP
Physical Chemistry Chemical Physics

Accepted Manuscript

This article can be cited before page numbers have been issued, to do this please use: A. Cotic, S. Cerfontaine, L. D. Slep, B. Elias, L. Troian-Gautier and A. Cadranel, *Phys. Chem. Chem. Phys.*, 2022, DOI: 10.1039/D2CP01791A.

ROYAL SOCIETY OF CHEMISTRY

rsc.li/pccp

View Article Online
DOI: 10.1039/D2CP01791A

ARTICLE

A Photoinduced Mixed Valence Photoswitch

Agustina Cotic,[a,b] Simon Cerfontaine,[c] Leonardo Slep,[a,b] Benjamin Elias,[c] Ludovic Troian-Gautier,[c] * and Alejandro Cadranel [a,b,d,e] *

Received 00th January 20xx,
Accepted 00th January 20xx

DOI: 10.1039/x0xx00000x

The ground state and photoinduced mixed valence states (GSMV and PIMV, respectively) of a dinuclear (Dp^{4+}) ruthenium(II) complex bearing 2,2'-bipyridine ancillary ligands and a 2,2':4',4'':2'',2'''-quaterpyridine (Lp) bridging ligand were investigated using femtosecond and nanosecond transient absorption spectroscopy, electrochemistry and density functional theory. It was shown that the electronic coupling between the transiently light-generated Ru(II) and Ru(III) centers is H_{DA} ~ 450 cm^{-1} in the PIMV state, whereas the electrochemically generated GSMV state showed H_{DA} ~ 0 cm^{-1}, despite virtually identical Ru-Ru distances. This stemmed from the changes in dihedral angles between the two bpy moieties of Lp, estimated at 30° and 4° for the GSMV and PIMV states, respectively, consistent with a through-bond rather than a through-space mechanism. Electronic coupling can be turned on by using visible light excitation, making Dp^{4+} a competitive candidate for photoswitching applications. A novel strategy to design photoinduced charge transfer molecular switches is proposed.

Introduction

In supramolecular donor-acceptor systems, electronic coupling (H_{DA}) regulates electron transport between different molecular fragments and other reactive processes.[1–5] Control over H_{DA} at the molecular level gives access to technologically relevant phenomena,[6] such as molecular wire behavior[7] and redox-[8–11] or photoswitching,[12–14] which can be applied in molecular electronics. Ground state mixed valence (GSMV) systems, where the same chemical fragment is present in different oxidations states, represent attractive models to study electronic coupling and electron transfer.[15–18] Indeed, via relatively simple techniques, such as UV-vis-NIR spectroscopy coupled to electrochemistry,[19] H_{DA} can be estimated by analysis of the shape and intensity of the ground state intervalence charge transfer absorption bands (GSIVCT) using the Mulliken-Hush expression (eq. 1).[20,21]

$$H_{DA} = 2.06 \times 10^{-2} \frac{\left(\nu_{max}\, \varepsilon_{max}\, \Delta\nu_{1/2}\right)^{1/2}}{r_{DA}} \quad (1)$$

Here, H_{DA} is the electronic coupling in cm^{-1}, ν_{max} is the energy in cm^{-1} of the band maximum, $\Delta\nu_{1/2}$ is the FWHM in cm^{-1} and r_{DA} is the distance between the donor and acceptor centroids in Å. This equation is valid for moderately coupled mixed valence systems, and derived H_{DA} values are lower limits since electronic coupling and wavefunction delocalization leads to real charge transfer distances that are shorter than physical r_{DA}.[4,16,22–25] However, for efficient photon and charge management in solar energy conversion schemes, control over H_{DA} *in the excited state* is necessary.[4] One approach involves the estimation of excited state redox potentials using ground-state electrochemical potentials plus the energy stored in the excited-state.[26] Alternatively, they can also be estimated by screening the photo-reactivity with a number of donor or acceptor counterparts.[27] In contrast, transient absorption spectroscopy (TAS) with NIR detection enables to directly study H_{DA} in the excited state by monitoring the photoinduced IVCT (PIIVCT) absorption bands, normally active in the NIR region.[28–32]

Polynuclear Ru(II) coordination complexes, widespread chromophores and photocatalysts, populate metal-to-ligand charge transfer (MLCT) excited states upon visible light excitation.[33–37] In a hypothetical bimetallic $\{Ru^{II}Ru^{II}(bpy)\}$ complex, population of a $\{Ru^{II}Ru^{III}(bpy^{\bullet-})\}$ MLCT state results in a transient $\{Ru^{II}Ru^{III}\}$ photoinduced mixed valence (PIMV) core that contains the excited hole.[4,38,39] The charge transfer counterpart, in this case the excited electron, is not directly engaged in PIMV interactions but is determinant for the properties of the system.[38,40–42] Polypyridines undergo significant structural rearrangements upon reduction,[43–49] resulting in semiquinoid or quinoid moieties where the dihedral angles between pyridinic rings are notably decreased in comparison to the non-reduced forms. For example, the dihedral angle of 4,4'-bpy has been theoretically calculated to

[a] Universidad de Buenos Aires, Facultad de Ciencias Exactas y Naturales, Departamento de Química Inorgánica, Analítica y Química Física, Pabellón 2, Ciudad Universitaria, C1428EHA, Buenos Aires, Argentina. E-mail: acadranel@qi.fcen.uba.ar
[b] CONICET – Universidad de Buenos Aires, Instituto de Química-Física de Materiales, Medio Ambiente y Energía (INQUIMAE), Pabellón 2, Ciudad Universitaria, C1428EHA, Buenos Aires, Argentina.
[c] Université catholique de Louvain (UCLouvain), Institut de la Matière Condensée et des Nanosciences (IMCN), Molecular Chemistry, Materials and Catalysis (MOST), Place Louis Pasteur 1, bte L4.01.02, 1348 Louvain-la-Neuve, Belgium. E-mail : Ludovic.Troian@uclouvain.be
[d] Friedrich-Alexander-Universität Erlangen-Nürnberg (FAU), Physical Chemistry I, Egerlandstr. 3, 91058, Erlangen, Germany.
[e] Friedrich-Alexander-Universität Erlangen-Nürnberg (FAU), Interdisciplinary Center for Molecular Materials, Egerlandstr. 3, 91058, Erlangen, Germany.
†Electronic Supplementary Information (ESI) available: Experimental details, calculations, nanosecond transient absorption spectroscopy. See DOI: 10.1039/x0xx00000x

View Article Online
DOI: 10.1039/D2CP01791A

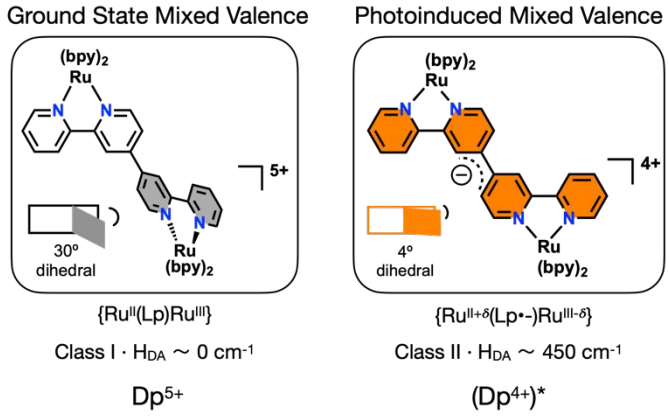

Figure 1. Structure of the ground state mixed valence and photoinduced mixed valence states of Dp^{n+} complexes studied herein, as well as their electronic configuration and their classification according to Robin and Day.

be 40.8°, and in solid compounds containing 4,4'-bpy it averages 18°, but in isolated compounds containing 4,4'-$bpy^{\bullet-}$ it averages below 3.2°.[50] Considering that coplanarity enhances wavefunction overlap, we hypothesized that in a bimetallic PIMV system bearing a judiciously designed polypyridine bridge, the presence of the excited electron on the bridge (BL) should have drastic effects on H_{DA} in the $\{Ru^{II}(BL^{\bullet-})Ru^{III}\}$ excited state. Hence, we selected a dinuclear ruthenium polypyridine photosensitizer (Dp^{n+}) (Figure 1), which is a $\{Ru(bpy)_3\}$ dimer with a bridging ligand connected via the *para* position (Lp) to the chelating nitrogen. This complex was studied both in the ground and excited states, using spectroelectrochemistry, nanosecond and femtosecond transient absorption spectroscopy (nsTAS and fsTAS, respectively) and DFT calculations. Here, we obtained clear experimental and theoretical evidence of significant electronic coupling in the $Lp^{\bullet-}$-bridged PIMV state, that was completely absent in the Lp-bridged GSMV state as inferred from (spectro)electrochemical mesurements.[51] Thus, Dp^{n+} represents a new class of molecular photoswitch, which relies on photoinduced charge transfer, rather than photoisomerizations,[12–14] to control electronic coupling between electroactive units at the molecular level, and can therefore be rationalized as a photo-triggered redox switch. Our results illustrate that the fundamental differences between ground state and photoinduced mixed valence systems can be leveraged for photon and charge management in general, and for the design of molecular photoswitches.

Results and Discussion

Dp^{4+} has a $\{Ru^{II}(Lp)Ru^{II}\}$ configuration and is exceptionally photostable, making it attractive for photocatalysis.[36] Previous investigations have focused on the ground and excited state properties of Dp^{4+}, but the key NIR region, and therefore Ru-Ru electronic coupling, was not studied.[52] Dp^{4+} presents typical MLCT absorptions in the visible, peaking at 481 nm in acetonitrile.[52] We first performed DFT and TDDFT calculations at the B3LYP level of theory employing a LanL2DZ basis set,

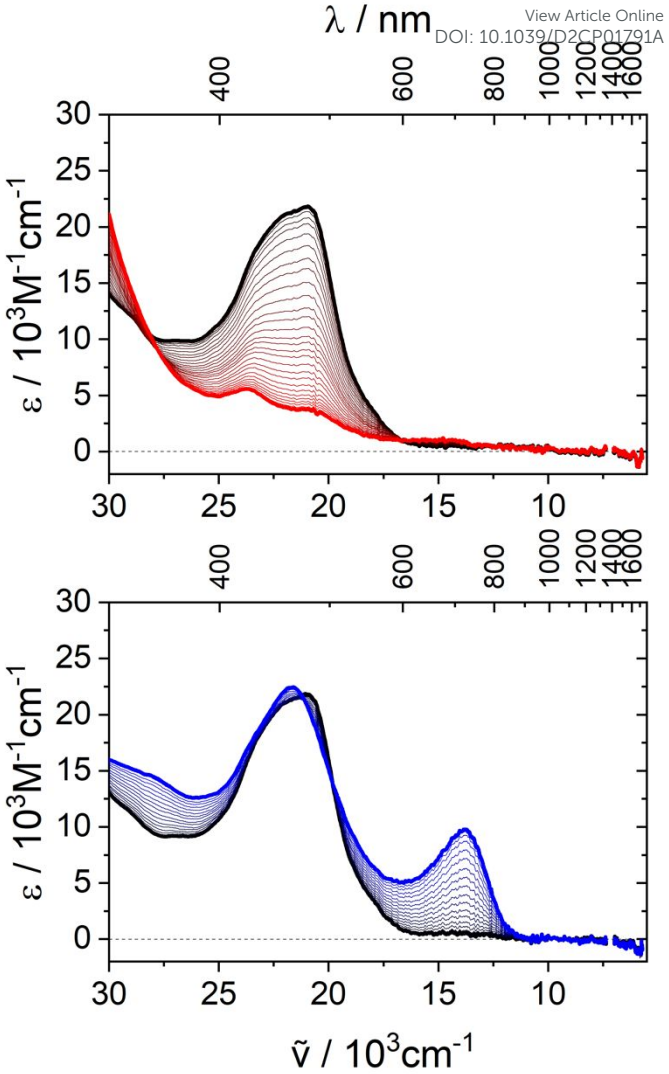

Figure 2. Spectroelectrochemical measurements recorded during the two-electron oxidation (top, potential scans from +1.2 to +1.5 V *vs.* Ag/AgCl) and one-electron reduction (bottom, potential scans from –0.8 to –1.15 V *vs.* Ag/AgCl) of Dp^{4+} in 0.1 M $TBAPF_6$ ACN electrolyte. Initial spectra (black) correspond to Dp^{4+} and the final spectra to Dp^{6+} (red) and Dp^{3+} (blue).

which is computationally cheaper than the def2SVP/6-31+G(d,p) basis sets.[52] Our results afford an excellent match with the experimental absorption spectrum in acetonitrile (Figure S1, Tables S1-S2). Electron density difference maps (EDDMs) of the most intense electronic transitions indicate that they are mostly of $d\pi(Ru)\rightarrow\pi^*(Lp)$ and $d\pi(Ru)\rightarrow\pi^*(bpy)$ character (Figure S2).

The GSMV state (Dp^{5+}) is the one-electron oxidized form of Dp^{4+}. Electrochemical experiments reveal that both Ru ions are oxidized at the same potential, featuring a single, two-electron wave, and resulting in the doubly oxidized $\{Ru^{III}(Lp)Ru^{III}\}$ species, Dp^{6+}.[51] Using spectroelectrochemistry, it was shown that oxidation of Dp^{4+} resulted in the decrease of the MLCT bands while the NIR region remains silent (Figure 2).[51] The absence of GSIVCT bands at every applied potential is consistent with no sizeable Ru-Ru electronic communication, or $H_{DA} \sim 0\ cm^{-1}$.[19,53–55] Therefore, the elusive Dp^{5+} intermediate species is a Class I ground state mixed valence system where the Ru ions are

View Article Online
DOI: 10.1039/D2CP01791A

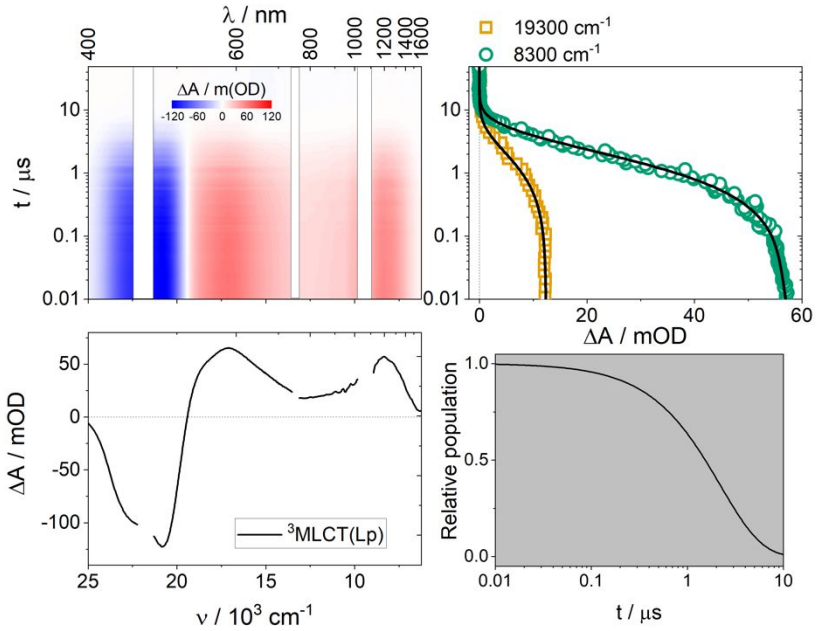

Figure 3. Top left: Differential absorption 3D map obtained from nsTAS for Dp^{4+} in ACN upon 460 nm (21700 cm^{-1}) excitation. Top right: Time absorption profile and corresponding fit at 8300 cm^{-1} and 19300 cm^{-1}. Bottom left: Species associated differential spectrum of the ^{3}MLCT(Lp) excited state. Bottom right: Concentration evolution over time.

electronically decoupled, with a completely localized $\{Ru^{II}(Lp)Ru^{III}\}$ electronic configuration.

The picture is very different in the MLCT excited state. $(Dp^{4+})^*$ shows emission at room temperature in ACN, with a maximum at 14660 cm^{-1}, and a photoluminescence lifetime of 2.35 μs.[52] Nanosecond TAS using 460 nm (21700 cm^{-1}) excitation with detection extended to the NIR was then used to address Ru-Ru excited state electronic coupling. Upon light absorption, two broad positive signals were detected at 17100 and 8340 cm^{-1}, respectively, that decay monotonically to zero (Figure 3). Global analysis of the data reveals only one exponential decay with a 2.21 μs lifetime, which matches the one previously observed for this ^{3}MLCT(Lp) state.[52] The high-energy photoinduced absorption centered at 17100 cm^{-1}, is ascribed to the bridging ligand radical anion, which, however, is NIR silent (Figure 2).[52] The low energy NIR features in $(Dp^{4+})^*$ are absent for the prototypical $[Ru(bpy)_3]^{2+}$ (Figure S3), therefore they must originate from the interaction between $\{Ru(bpy)_3\}$ fragments and are ascribed to PIIVCT absorptions. Similar NIR bands have been observed for related bimetallic ruthenium polypyridines.[28,38–40] This indicates that $(Dp^{4+})^*$ is a PIMV system, with a $\{Ru^{II+\delta}(Lp^{\bullet-})Ru^{III-\delta}\}$ electronic configuration. In other words, the Ru ions are electronically coupled in the excited state.

DFT and TDDFT calculations on the lowest triplet state confirmed our assignments of a ^{3}MLCT(Lp) state. A corresponding orbital transformation (COT)[56,57] of the DFT calculated electronic structure reveals the location of the unpaired electrons (the excited hole-electron pair) in the MLCT state (Figure 4). The excited electron lies on the bridging ligand, consistent with reductive spectroelectrochemical experiments (Figure 2) [51] whereas the excited hole is mostly localized on one of the Ru ions. The calculated electronic transitions yield an excellent coincidence with the experimental nanosecond transient absorption spectrum (Figure 4, Tables S3-S4), as in other bimetallic ruthenium polypyridines showing PIIVCT absorptions.[28,40] First, an intense transition ($f > 0.1$) is calculated at 19157 cm^{-1} (#34), which, together with less intense transitions down to 11000 cm^{-1}, reproduces the broad photoinduced absorption that extends from 19300 to 11100 cm^{-1}. An additional transition is calculated at 22672 cm^{-1} (#53), but it is located close to the ground state bleach region. According to their EDDMs, these are of π*(Lp)→π*(bpy) and dπ(Ru)→π*(bpy) character (Figure S4 and Table S3). Furthermore, two very intense transitions ($f > 0.1$) are calculated in the NIR, at 7185 (#6) and 7904 cm^{-1} (#7), respectively, matching the experimental PIIVCT band at 8340 cm^{-1}. The transition involving the excited state #7 is mostly H-1(B)→LUMO(B) (74%) in character (Table S3), and the EDDM surface clearly shows it is a PIIVCT (Figure S4). This transition can be seen as a "clean" Ru-Ru CT over a distance of 11.318 Å, keeping the electron density due to the excited electron on the bridge roughly frozen at the lowest energy triplet state distribution. The transition involving the excited state #6 arises from the superposition of three different contributions. The resulting state is in part PIIVCT in character due to the H-1(B)→LUMO(B) (21%) and HOMO(B)→LUMO(B) (22%) contributions, but also has a substantial π-π* composition (Figure S4 and Table S3). Altogether, it seems to be a second PIIVCT' state in which the electron density of the bridge accompanies the movement of the electron from one metal center to the other. Both transitions are consistent with a mostly localized nature of the excited hole in the MLCT state, revealed by the COT analysis (Figure 4).

View Article Online DOI: 10.1039/D2CP01701F

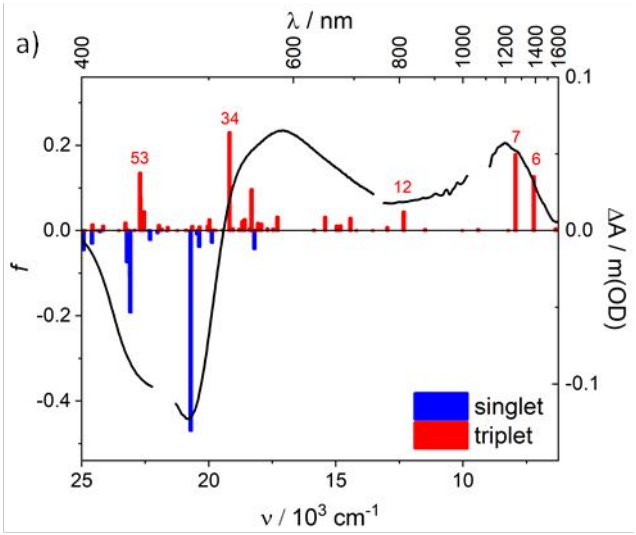

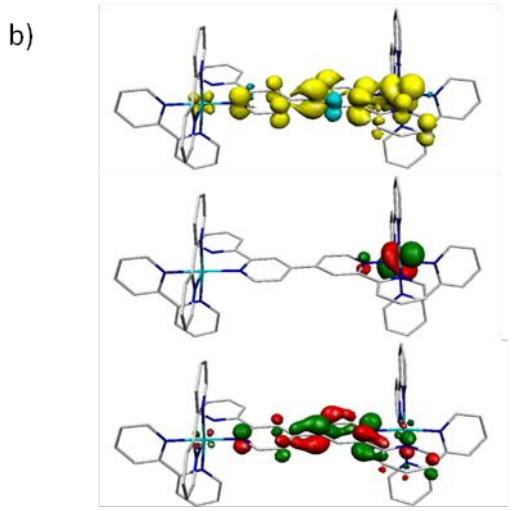

Figure 4. a) Calculated electronic transitions for the singlet and triplet states of Dp^{4+}, and experimental differential spectrum of the ^{3}MLCT(Lp) state. b) Spin density (top) and SOMOs (middle, bottom) for the lowest energy triplet state of Dp^{4+} computed after a COT.

Therefore, the calculated electronic structure is a good description of the PIMV system, which belongs to Robin and Day's Class II.[53]

Quantification of H_{DA} in $(Dp^{4+})^*$ following a "classical" Marcus-Hush treatment of the PIIVCT transition or a more elaborated "several states" approach as we employed before[58] is difficult. On the one hand, there is a considerable non charge-transfer, π-π* mixed character of one of the observed transitions. On the other hand, if the same superexchange mechanism as in pyrazine and 4,4'-bpy-bridged systems is operative (*vide infra*), it turns into, at least, a four-state problem, since $^3\{Ru^{III}(Lp^{2-})Ru^{III}\}$ and ^{3}LF $\{Ru^{II}*(Lp)Ru^{II}\}$ or $\{Ru^{II}(Lp)Ru^{II}*\}$ states are involved, besides ^{3}MLCT $\{Ru^{II}(Lp^{\bullet-})Ru^{III}\}$ and $\{Ru^{III}(Lp^{\bullet-})Ru^{II}\}$, in the donor-acceptor mixed valence interaction. The absence of clear experimental observation of those additional states precludes any attempt to extract quantitative information. A simpler alternative could involve the deconvolution of the strongly overlapping low energy transitions using Gaussian profiles for the fit, and individual analyses of each transition according to Mulliken-Hush.[22,59] This can be achieved if the molar extinction coefficients of the ^{3}MLCT(Lp) excited state, rather than those of the ground state, are known. Spectroelectrochemistry is thus not useful to this end but the excited state extinction coefficients can be obtained by comparison of the transient absorption spectrum of Dp^{4+} with that of $[Ru(bpy)_3]^{2+}$, under the same laser conditions.[60] Thus, we measured nsTAS in the UV-vis-NIR range using 460 nm (21700 cm^{-1}) excitation for both Dp^{4+} (Figure 3) and $[Ru(bpy)_3]^{2+}$ (Figure S3). This strategy is strictly valid only if the quantum efficiencies for the population of the lowest triplet state (η_T) are known in both cases. For $[Ru(bpy)_3]^{2+}$, it is known that $\eta_T \sim 1$.[61] The excited-state decay cascade of Dp^{4+} is similar to that of $[Ru(bpy)_3]^{2+}$, since the quantum efficiencies for intersystem crossing are expected to be unitary, and the only excited state activity registered in femtosecond TAS (fsTAS) of Dp^{4+} (Figure S5) is a vibrational cooling process. This implies that $\eta_T \sim 1$ for Dp^{4+}, allowing the determination of molar extinction coefficient by comparative actinometry. Using $[Ru(bpy)_3]^{2+}$ as a reference, the transient spectrum of $(Dp^{4+})^*$ was converted from m(OD) to Δε units,[60] representing the difference of the extinction molar coefficient of the excited state minus that of the ground state. Given that the ground state of Dp^{4+} doesn't present NIR features, then, in this region, Δε = ε(PIIVCT). This is important since the Mulliken-Hush treatment uses ε and not Δε. After units conversion, the NIR differential spectrum of $(Dp^{4+})^*$ was deconvoluted using three Gaussian functions (Figure 5). The highest energy Gaussian (ν_{max} = 11876 cm^{-1}, ε_{max} = 2201 $M^{-1}cm^{-1}$, $\Delta\nu_{1/2}$ = 6065 cm^{-1}) can be assigned to a mixture of π*-π* within $Lp^{\bullet-}$ and a π*(Lp)→ π*(bpy) LL'CT (calculated transition #12 at 12304 cm^{-1}, Figures 4 and S6). The other two Gaussians (ν_{max} = 8988 cm^{-1}, ε_{max} = 2915 $M^{-1}cm^{-1}$, $\Delta\nu_{1/2}$ = 2507 cm^{-1}, and ν_{max} = 7906 cm^{-1}, ε_{max} = 3466 $M^{-1}cm^{-1}$, $\Delta\nu_{1/2}$ = 1768 cm^{-1}, respectively) are ascribed to PIIVCT transitions (calculated transitions #6 and #7). Using the spectral parameters of PIIVCT Gaussians and a DFT calculated donor acceptor distance of 11.3 Å in equation (1), H_{DA} = 400 cm^{-1} and 465 cm^{-1} according to each Gaussian, respectively. These values are modest for Class II mixed valence systems,[53,62–64] and are fully consistent with a mostly localized configuration of the excited hole.

DFT-calculated Ru-Ru distances in Dp^{4+} (11.314 Å) and in $(Dp^{4+})^*$ (11.318 Å) were too similar to explain the observed contrasting experimental behavior. However, while Lp considerably deviates from planarity with a dihedral angle of 30° in Dp^{4+}, $Lp^{\bullet-}$ is almost perfectly planar with an angle of 4° in $(Dp^{4+})^*$. These differences are commonly observed in polypyridine-type ligands upon reduction, and show the prevalence of a semiquinoid form in the radical anionic state.[43–49] In the related $[Ru(dpb)_3]^{2+}$, where dpb is 4,4'-diphenyl-2,2'-bipyridine, planarization of dpb in the MLCT excited states leads to extended delocalization and prolonged lifetimes in comparison to $[Ru(bpy)_3]^{2+}$.[65] The drastic consequences that planarization of the bridging ligand has on Ru-Ru electronic coupling while these ions are kept at virtually identical distances is consistent with through-bond rather than through-space interactions, with an active participation of Lp-centered orbitals and a bridge-mediated superexchange mechanism.[21,66] The structural

analogy between Lp and 4,4'-bpy is crucial in determining the photoswitching behavior of Dp^{n+}. These bridging ligands are based on biphenyl moieties, where the coordinating sites for each electroactive unit (each 2,2'-bpy in Lp, or each pyridine in 4,4'-bpy) are separated and can rotate with respect to the other. In contrast, when the bridging ligand is structurally analogous to 2,2'-bpy or pyrazine, like 2,2'-bipyrimidine, 2,3-Di-(2-pyridin)pyrazyl,[67,68] 2,3,5,6-tetrakis(2-pyridyl)pyrazine,[29] or pyrazine itself,[30] the coordinating sites are not separated or rotation is impeded. In these cases, the radical anionic forms of the bridges promote similar electronic couplings than their non-reduced forms, hampering any use as photoswitches.

The performance of Dp^{4+} as a photoswitch is based on the interconversion of electromers (electronic isomers) with different absorption spectra, i.e. the ground state and the MLCT(Lp) state (Figure 6), instead of other types of isomers as in traditional photoswitches. Any visible light that is absorbed by Dp^{4+} leads to the formation of the same MLCT(Lp) state, therefore any visible light input is useful for promoting GS→MLCT(Lp) and switching electronic coupling. GS→MLCT(Lp) photoconversion yields are approximately 100 %, because, as discussed above, $\eta_T \sim 1$ for Dp^{4+}, and no triplets other than MLCT(Lp) were detected in fsTAS (Figure S5). The thermal reversibility is characterized by the MLCT(Lp)→GS lifetime of 2.21 μs. This is an important parameter that should be tuned according to the desired application. Importantly, this system does not present any evidence of fatigue at room temperature. This stems from very high activation energies required for the population of MC states,[52] which represent the only known reaction pathway that could potentially lead to photodecompostion. While long-term experiments are beyond the scope of this study, routinary fsTAS experiment involves three consecutive scans that take approximately 8 minutes each, under 460 nm excitation at 1 kHz and 500 nJ per pulse. During the course of these experiments, no significant changes in the transient absorption spectra nor the steady state absorption spectra of Dp^{4+} were detected. Therefore, Dp^{4+} shows virtually full reversibility of the on-off (excitation-decay) cycles.

Finally, it is worth to point out that it is impossible to prepare PIMV systems like $\{Ru^{II+\delta}(Lp^{\bullet-})Ru^{III-\delta}\}$ using only redox inputs, since the reduction potential of the bridging ligand and the oxidation potential of the Ru ions are incompatible. Therefore, the experimental determination of the electronic coupling promoted by the reduced bridge is an asset exclusive of PIMV systems.

Conclusions

In conclusion, in the $\{Ru(bpy)_3\}$ dimer Dp^{n+}, which benefits from an excellent photostability and full reversibility of excitation-decay (on-off) cycles, electronic coupling can be turned on by using visible light inputs. We demonstrated the implementation of photoinduced mixed valence interactions in the design of molecular photoswitches. This should be guided by the judicious design of bridging ligands, which determine ground and excited state electronic couplings via the fundamental differences of GSMV and PIMV systems.

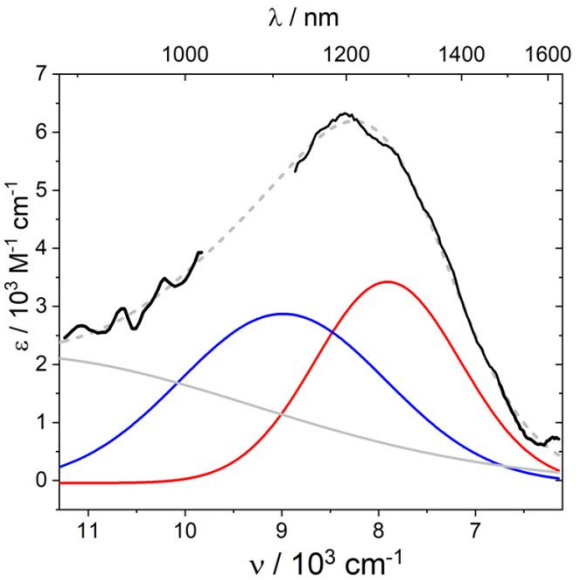

Figure 5. Gaussian deconvolution of the transient NIR differential absorption of Dp^{4+*} (black curve) by three gaussians (grey, blue and red solid curves). The convoluted spectrum is shown as a grey dashed curve

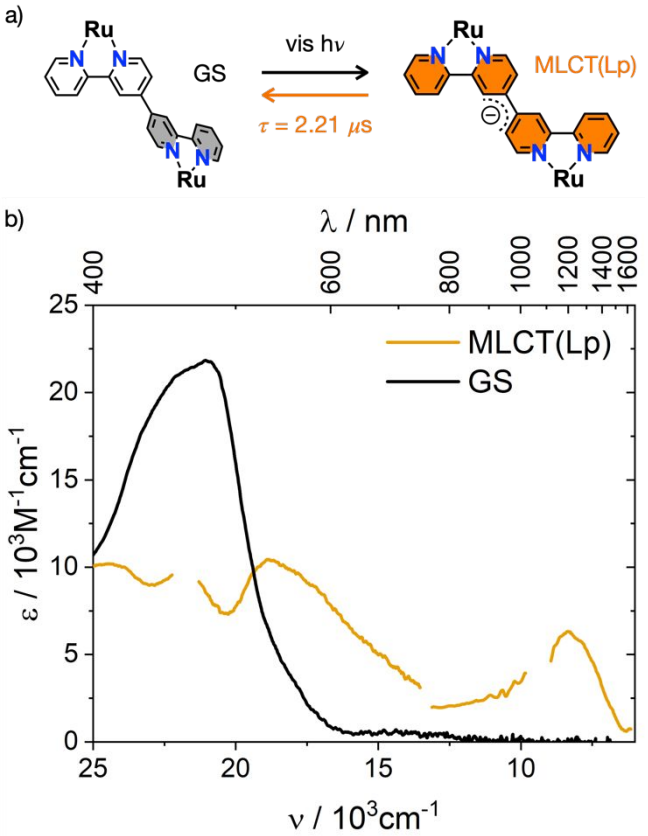

Figure 6. a) Photoswitching behavior of Dp^{4+}. Any visible light input populates MLCT(Lp) state, which returns back to the ground state with a microsecond lifetime. b) Absorption spectra of the ground state (GS) and the MLCT(Lp) state of Dp^{4+} in acetonitrile at room temperature. MLCT(Lp) absorption spectrum was reconstructed from the differential transient absorption spectrum plus the ground state absorption spectrum.

Conflicts of interest

There are no conflicts to declare.

Acknowledgements

A. Cotic thanks CONICET for a doctoral fellowship. S. C. and B. E. gratefully acknowledge the UCLouvain for financial support. L. T.-G. is a collaborateur scientifique of the Fonds de la Recherche Scientifique – FNRS. A. Cadranel is a member of the research staff of CONICET and an ALN associate. A. Cadranel thanks Dirk Guldi for providing access to ultrafast spectroscopy facilities. Funding from ANPCyT (PICT 2018-00924 and 2019-02410) and CONICET (PIP 11220200102757CO) is gratefully acknowledged (A. Cadranel).

Notes and references

1 J. R. Winkler and H. B. Gray, Electron flow through metalloproteins, *Chem. Rev.*, 2014, **114**, 3369–3380.
2 K. D. Jordan and M. N. Paddon-Row, Analysis of the Interactions Responsible for Long-Range Through-Bond-Mediated Electronic Coupling between Remote Chromophores Attached to Rigid Polynorbornyl Bridges, *Chem. Rev.*, 1992, **92**, 395–410.
3 M. Manathunga, X. Yang and M. Olivucci, Electronic State Mixing Controls the Photoreactivity of a Rhodopsin with all-trans Chromophore Analogues, *J. Phys. Chem. Lett.*, 2018, **9**, 6350–6355.
4 R. N. Sampaio, E. J. Piechota, L. Troian-Gautier, A. B. Maurer, K. Hu, P. A. Schauer, A. D. Blair, C. P. Berlinguette and G. J. Meyer, Kinetics teach that electronic coupling lowers the free-energy change that accompanies electron transfer, *Proc. Natl. Acad. Sci.* , 2018, **115**, 7248–7253.
5 O. S. Wenger, How Donor - Bridge - Acceptor energetics influence electron tunneling dynamics and their distance dependences, *Acc. Chem. Res.*, 2011, **44**, 25–35.
6 H. Chen and J. Fraser Stoddart, From molecular to supramolecular electronics, *Nat. Rev. Mater.*, 2021, **6**, 804–828.
7 P. J. Low, Twists and turns: Studies of the complexes and properties of bimetallic complexes featuring phenylene ethynylene and related bridging ligands, *Coord. Chem. Rev.*, 2013, **257**, 1507–1532.
8 Y. Li, M. Baghernejad, A. G. Qusiy, D. Zsolt Manrique, G. Zhang, J. Hamill, Y. Fu, P. Broekmann, W. Hong, T. Wandlowski, D. Zhang and C. Lambert, Three-State Single-Molecule Naphthalenediimide Switch: Integration of a Pendant Redox Unit for Conductance Tuning, *Angew. Chem.Int.Ed.*, 2015, **54**, 13586–13589.
9 F. Meng, Y. M. Hervault, Q. Shao, B. Hu, L. Norel, S. Rigaut and X. Chen, Orthogonally modulated molecular transport junctions for resettable electronic logic gates, *Nat. Commun.*, 2014, **5**, 1–9.
10 Y. Oyama, R. Kawano, Y. Tanaka and M. Akita, Dinuclear ruthenium acetylide complexes with diethynylated anthrahydroquinone and anthraquinone frameworks a multi-stimuli-responsive organometallic switch, *Dalton Trans.*, 2019, **48**, 7432–7441.
11 L. Norel, C. Tourbillon, J. Warnan, J. F. Audibert, Y. Pellegrin, F. Miomandre, F. Odobel and S. Rigaut, Redox-driven porphyrin based systems for new luminescent molecular switches, *Dalton Trans.*, 2018, **47**, 8364–8374.
12 O. S. Wenger, Photoswitchable mixed valence, *Chem. Soc. Rev.*, 2012, **41**, 3772–3779.
13 J. Andréasson and U. Pischel, Light-stimulated molecular and supramolecular systems for information processing and beyond, *Coord. Chem. Rev.*, 2021, **429**, 213695.
14 J. Volarić, W. Szymanski, N. A. Simeth and B. L. Feringa, Molecular photoswitches in aqueous environments, *Chem. Soc. Rev.*, 2021, **50**, 12377–12449.
15 C. Creutz and H. Taube, A Direct Approach to Measuring the Franck-Condon Barrier to Electron Transfer between Metal Ions, *J. Am. Chem. Soc.*, 1969, **91**, 3988–3989.
16 E. J. Piechota and G. J. Meyer, Introduction to Electron Transfer: Theoretical Foundations and Pedagogical Examples, *J. Chem. Educ.*, 2019, **96**, 2450–2466.
17 M. J. Powers and T. J. Meyer, Intervalence transfer in the mixed-valence ion $[(bpy)_2(py)Ru(4,4'\text{-}bpy)Ru(py)(bpy)_2]^{5+}$, *Inorg. Chem.*, 1978, **17**, 1785–1790.
18 C. H. Londergan, J. C. Salsman, B. J. Lear and C. P. Kubiak, Observation and dynamics of 'mixed-valence isomers' and a thermodynamic estimate of electronic coupling parameters, *Chem. Phys.*, 2006, **324**, 57–62.
19 R. F. Winter, Half-wave potential splittings δE1/2 as a measure of electronic coupling in mixed-valent systems: Triumphs and defeats, *Organometallics*, 2014, **33**, 4517–4536.
20 B. S. Brunschwig, C. Creutz and N. Sutin, Optical transitions of symmetrical mixed-valence systems in the class II-III transition regime, *Chem. Soc. Rev.*, 2002, **31**, 168–184.
21 E. J. Piechota, L. Troian-Gautier, R. N. Sampaio, M. K. Brennaman, K. Hu, C. P. Berlinguette and G. J. Meyer, Optical Intramolecular Electron Transfer in Opposite Directions through the Same Bridge That Follows Different Pathways, *J. Am. Chem. Soc.*, 2018, **140**, 7176–7186.
22 R. J. Cave and M. D. Newton, Generalization of the Mulliken-Hush treatment for the calculation of electron transfer matrix elements, *Chem. Phys. Lett.*, 1996, **249**, 15–19.
23 L. Karki and J. T. Hupp, Orbital specific charge transfer distances, solvent reorganization energies, and electronic coupling energies: Electronic stark effect studies of parallel and orthogonal intervalence transfer in $(NC)_5Os(II)\text{-}CN\text{-}Ru(III)(NH_3)^{5-}$, *J. Am. Chem. Soc.*, 1997, **119**, 4070–4073.
24 D. H. Oh, M. Sano and S. G. Boxer, Electroabsorption (Stark effect) spectroscopy of mono- and biruthenium charge-transfer complexes: measurements of changes in dipole moments and other electrooptic properties, *J. Am. Chem. Soc.*, 1991, **113**, 6880–6890.
25 E. J. Piechota, R. N. Sampaio, L. Troian-Gautier, A. B. Maurer, C. P. Berlinguette and G. J. Meyer, Entropic Barriers Determine Adiabatic Electron Transfer Equilibrium, *J. Phys. Chem. C*, 2019, **123**, 3416–3425.
26 D. W. Thompson, A. Ito and T. J. Meyer, $[Ru(bpy)_3]^{2+*}$ and other remarkable metal-to-ligand charge transfer (MLCT) excited states, *Pure Appl. Chem.*, 2013, **85**, 1257–1305.
27 M. D. Woodhouse and J. K. McCusker, Mechanistic Origin of

Photoredox Catalysis Involving Iron(II) Polypyridyl Chromophores, *J. Am. Chem. Soc.*, 2020, **142**, 16229–16233.

28 P. S. Oviedo, G. E. Pieslinger, L. M. Baraldo, A. Cadranel and D. M. Guldi, Coexistence of MLCT Excited States of Different Symmetry upon Photoexcitation of a Single Molecular Species, *J. Phys. Chem. C*, 2019, **123**, 3285–3291.

29 D. M. Dattelbaum, C. M. Hartshorn and T. J. Meyer, Direct Measurement of Excited-State Intervalence Transfer in $[(tpy)Ru^{III}(tppz\bullet^-)Ru^{II}(tpy)]^{4+*}$ by Time-Resolved Near-Infrared Spectroscopy, *J. Am. Chem. Soc.*, 2002, **124**, 4938–4939.

30 C. N. Fleming, D. M. Dattelbaum, D. W. Thompson, A. Y. Ershov and T. J. Meyer, Excited state intervalence transfer in a rigid polymeric film, *J. Am. Chem. Soc.*, 2007, **129**, 9622–9630.

31 K. Matsui, M. K. Nazeeruddin, R. Humphry-Baker, M. Grätzel and K. Kalyanasundaram, Transient absorptions due to mixed valence species in the excited-state absorption spectra of cyano-bridged trinuclear polypyridyl complexes of Ru(II), *J. Phys. Chem.*, 1992, **96**, 10587–10590.

32 J. B. G. Gluyas, A. N. Sobolev, E. G. Moore and P. J. Low, Broad-Band NIR Transient Absorption Spectroscopy of an 'All-Carbon'-Bridged Bimetallic Radical Cation Complex, *Organometallics*, 2015, **34**, 3923–3926.

33 V. Balzani, G. Bergamini, P. Ceroni and E. Marchi, Designing light harvesting antennas by luminescent dendrimers, *New J. Chem.*, 2011, **35**, 1944–1954.

34 A. Juris, V. Balzani, F. Barigelletti, S. Campagna, P. Belser and A. von Zelewsky, Ru(II) polypyridine complexes: photophysics, photochemistry, eletrochemistry, and chemiluminescence, *Coord. Chem. Rev.*, 1988, **84**, 85–277.

35 S. Serroni, S. Campagna, F. Puntoriero, C. Di Pietro, N. D. Mc Clenaghan and F. Loiseau, Dendrimers based on ruthenium(II) and osmium(II) polypyridine complexes and the approach of using complexes as ligands and complexes as metals, *Chem. Soc. Rev.*, 2001, **30**, 367–375.

36 S. Cerfontaine, S. A. M. Wehlin, B. Elias and L. Troian-Gautier, Photostable Polynuclear Ruthenium(II) Photosensitizers Competent for Dehalogenation Photoredox Catalysis at 590 nm, *J. Am. Chem. Soc.*, 2020, **142**, 5549–5555.

37 S. Cerfontaine, L. Troian-Gautier, Q. Duez, J. Cornil, P. Gerbaux and B. Elias, MLCT Excited-State Behavior of Trinuclear Ruthenium(II) 2,2′-Bipyridine Complexes, *Inorg. Chem.*, 2021, **60**, 366–379.

38 B. M. Aramburu-Trošelj, P. S. Oviedo, I. Ramírez-Wierzbicki, L. M. Baraldo and A. Cadranel, Inversion of donor-acceptor roles in photoinduced intervalence charge transfers, *Chem. Commun.*, 2019, **55**, 7659–7662.

39 P. S. Oviedo, L. M. Baraldo and A. Cadranel, Bifurcation of excited state trajectories toward energy transfer or electron transfer directed by wave function symmetry, *Proc. Natl. Acad. Sci.*, 2021, **118**, e2018521118.

40 B. M. Aramburu-Trošelj, P. S. Oviedo, G. E. Pieslinger, J. H. Hodak, L. M. Baraldo, D. M. Guldi and A. Cadranel, A Hole Delocalization Strategy: Photoinduced Mixed-Valence MLCT States Featuring Extended Lifetimes, *Inorg. Chem.*, 2019, **58**, 10898–10904.

41 C. A. Bignozzi, R. Argazzi, C. Chiorboli, F. Scandola, R. B. Dyer, J. R. Schoonover and T. J. Meyer, Vibrational and Electronic Spectroscopy of Electronically Excited Polychromophoric Ruthenium(II) Complexes, *Inorg. Chem.*, 1994, **33**, 1652–1659.

42 C. A. Bignozzi, S. Roffia, C. Chiorboli, J. Davila, M. T. Indelli and F. Scandola, Oligomeric Dicyanobis(polypyridine)ruthenium(II) Complexes. Synthesis and Spectroscopic and Photophysical Properties, *Inorg. Chem.*, 1989, **28**, 4350–4358.

43 H. Kihara and Y. Gondo, Resonance Raman spectrum of the 4, 4′-bipyridine radical anion, *J. Raman Spectrosc.*, 1986, **17**, 263–267.

44 M. Wang, T. Weyhermüller, J. England and K. Wieghardt, Molecular and Electronic Structures of Six-Coordinate "Low-Valent" $[M(Mebpy)_3]^0$ (M = Ti, V, Cr, Mo) and $[M(tpy)_2]^0$ (M = Ti, V, Cr), and Seven-Coordinate $[MoF(Mebpy)_3](PF_6)$ and $[MX(tpy)_2](PF_6)$ (M = Mo, X = Cl and M = W, X = F), *Inorg. Chem.*, 2013, **52**, 12763–12776.

45 A. C. Bowman, J. England, S. Sproules, T. Weyhermüller and K. Wieghardt, Electronic Structures of Homoleptic [Tris(2,2′-bipyridine)M]^n Complexes of the Early Transition Metals (M = Sc, Y, Ti, Zr, Hf, V, Nb, Ta; n = 1+, 0, 1–, 2–, 3–): An Experimental and Density Functional Theoretical Study, *Inorg. Chem.*, 2013, **52**, 2242–2256.

46 J.-C. Berthet, P. Thuéry and M. Ephritikhine, Thorocene adducts of the neutral 2,2′-bipyridine and its radical anion. Synthesis and crystal structures of $[Th(\eta^8\text{-}C_8H_8)_2(\kappa^2\text{-bipy})]$ and $[Th(\mu\text{-}\eta^8\text{:}\eta^5\text{-}C_8H_8)_2(\kappa^2\text{-bipy})K(py)_2]_\infty$, *Comptes Rendus Chim.*, 2014, **17**, 526–533.

47 S. DeCarlo, D. H. Mayo, W. Tomlinson, J. Hu, J. Hooper, P. Zavalij, K. Bowen, H. Schnöckel and B. Eichhorn, Synthesis, Structure, and Properties of $Al(Rbpy)_3$ Complexes (R = t -Bu, Me): Homoleptic Main-Group Tris-bipyridyl Compounds, *Inorg. Chem.*, 2016, **55**, 4344–4353.

48 A. Formanuik, F. Ortu, J. Liu, L. E. Nodaraki, F. Tuna, A. Kerridge and D. P. Mills, Double Reduction of 4,4′-Bipyridine and Reductive Coupling of Pyridine by Two Thorium(III) Single-Electron Transfers, *Chem. - A Eur. J.*, 2017, **23**, 2290–2293.

49 M. Wang, J. England, T. Weyhermüller and K. Wieghardt, Molecular and Electronic Structures of the Members of the Electron Transfer Series $[Mn(bpy)_3]^n$ (n = 2+, 1+, 0, 1−) and $[Mn(tpy)_2]^m$ (m = 4+, 3+, 2+, 1+, 0). An Experimental and Density Functional Theory Study, *Inorg. Chem.*, 2014, **53**, 2276–2287.

50 M. S. Denning, M. Irwin and J. M. Goicoechea, Synthesis and characterization of the 4,4′-bipyridyl dianion and radical monoanion. A structural study, *Inorg. Chem.*, 2008, **47**, 6118–6120.

51 Y. Halpin, L. Cleary, L. Cassidy, S. Horne, D. Dini, W. R. Browne and J. G. Vos, Spectroelectrochemical properties of homo- and heteroleptic ruthenium and osmium binuclear complexes: intercomponent communication as a function of energy differences between HOMO levels of bridge and metal centres, *Dalton Trans.*, 2009, 4146.

52 S. Cerfontaine, L. Troian-Gautier, S. A. M. Wehlin, F. Loiseau, E. Cauët and B. Elias, Tuning the excited-state deactivation pathways of dinuclear ruthenium(II) 2,2′-bipyridine complexes through bridging ligand design, *Dalton Trans.*, 2020, **49**, 8096–8106.

53 M. B. Robin and P. Day, in *Advances in Inorganic Chemistry and Radiochemistry*, 1968, vol. 10, pp. 247–422.

View Article Online
DOI: 10.1039/D2CP01791A

54 M. Parthey and M. Kaupp, Quantum-chemical insights into mixed-valence systems: Within and beyond the Robin-Day scheme, *Chem. Soc. Rev.*, 2014, **43**, 5067–5088.
55 J. Hankache and O. S. Wenger, Organic mixed valence, *Chem. Rev.*, 2011, **111**, 5138–5178.
56 F. Neese, Definition of corresponding orbitals and the diradical character in broken symmetry DFT calculations on spin coupled systems, *J. Phys. Chem. Solids*, 2004, **65**, 781–785.
57 H. F. King, R. E. Stanton, H. Kim, R. E. Wyatt and R. G. Parr, Corresponding orbitals and the nonorthogonality problem in molecular quantum mechanics, *J. Chem. Phys.*, 1967, **47**, 1936–1941.
58 P. Alborés, M. B. Rossi, L. M. Baraldo and L. D. Slep, Donor-acceptor interactions and electron transfer in cyano-bridged trinuclear compounds, *Inorg. Chem.*, 2006, **45**, 10595–10604.
59 M. Rust, J. Lappe and R. J. Cave, Multistate effects in calculations of the electronic coupling element for electron transfer using the generalized Mulliken-Hush method, *J. Phys. Chem. A*, 2002, **106**, 3930–3940.
60 P. Müller and K. Brettel, $[Ru(bpy)_3]^{2+}$ as a reference in transient absorption spectroscopy: Differential absorption coefficients for formation of the long-lived 3MLCT excited state, *Photochem. Photobiol. Sci.*, 2012, **11**, 632–636.
61 N. H. Damrauer, G. Cerullo, A. Yeh, T. R. Boussie, C. V. Shank and J. K. McCusker, Femtosecond Dynamics of Excited-State Evolution in $[Ru(bpy)_3]^{2+}$, *Science*, 1997, **275**, 54–57.
62 M. D. Ward, Metal-metal interactions in binuclear complexes exhibiting mixed valency; molecular wires and switches, *Chem. Soc. Rev.*, 1995, **24**, 121–134.
63 D. M. D'Alessandro and F. R. Keene, Intervalence charge transfer (IVCT) in trinuclear and tetranuclear complexes of iron, ruthenium, and osmium, *Chem. Rev.*, 2006, **106**, 2270–2298.
64 L. T. Zhang, X. Q. Zhu, S. M. Hu, Y. X. Zhang, S. D. Su, Y. Y. Yang, X. T. Wu and T. L. Sheng, Influence of ligand substitution at the donor and acceptor center on MMCT in a cyanide-bridged mixed-valence system, *Dalton Trans.*, 2019, **48**, 7809–7816.
65 N. H. Damrauer, T. R. Boussie, M. Devenney and J. K. McCusker, Effects of Intraligand Electron Delocalization, Steric Tuning, and Excited-State Vibronic Coupling on the Photophysics of Aryl-Substituted Bipyridyl Complexes of Ru(II), *J. Am. Chem. Soc.*, 1997, **119**, 8253–8268.
66 K. Hu, A. D. Blair, E. J. Piechota, P. A. Schauer, R. N. Sampaio, F. G. L. Parlane, G. J. Meyer and C. P. Berlinguette, Kinetic pathway for interfacial electron transfer from a semiconductor to a molecule, *Nat. Chem.*, 2016, **8**, 853–859.
67 Y. J. Chen, J. F. Endicott and V. Swayambunathan, Emission band shape probes of the mixed-valence excited state properties of polypyridyl-bridged bis-ruthenium(II) complexes, *Chem. Phys.*, 2006, **326**, 79–96.
68 J. F. Endicott and Y. J. Chen, Observations concerning light promoted electronic delocalization in covalently linked transition metal complexes, *Inorganica Chim. Acta*, 2007, **360**, 913–922.